ELSEVIER

Materials Science and Engineering B91–92 (2002) 529–533

MATERIALS SCIENCE & ENGINEERING B

www.elsevier.com/locate/mseb

Study of the defect structure, compositional and electrical properties of Er_2O_3-doped n-type GaSb:Te crystals grown by the vertical Bridgman technique

J.L. Plaza [a,*], P. Hidalgo [b], B. Mendez [b], J. Piqueras [b], E. Dieguez [a]

[a] *Departamento de Fisica de Materiales, Facultad de Ciencias, Universidad Autonoma de Madrid, Cantoblanco, 28049 Madrid, Spain*
[b] *Departamento de Fisica de Materiales, Facultad de Fisicas, Universidad Complutense de Madrid, 28040 Madrid, Spain*

Abstract

The defect structure of Te-doped GaSb samples co-doped with Er_2O_3 and grown by the vertical Bridgman technique has been analysed. This study was carried out for different Er and Te concentrations. The defect structure of the samples has been analysed by means of cathodoluminescence (CL), scanning electron microscopy (SEM) and wavelength dispersive X-ray microanalysis (WDX). The effect of the defect structure and sample composition on the electrical properties of the material has been established taking into account the results obtained by means of the van der Pauw technique.

Keywords: Gallium antimonide; Doping effects; Tellurium; CL; WDX

1. Introduction

In the last decades there has been an increasing interest in the study of the physical properties of rare earth (RE)-doped semiconductors. It can be realised that the applications of materials that contain RE ions are not only restricted to the field of laser media but also play a key role in the field of semiconductor light-emitting devices [1].

The RE ions are found as trivalent ions in the most interesting crystals. It is the singular electronic structure of the RE ions which is responsible of their unique spectroscopic properties [2]. The emissions coming from the optically active 4f shell are almost unperturbed by the environment because the screening effect of the outer shells $5s^2$ and $5p^6$. In this way, many of the optical properties, which can be observed in RE-doped crystals and, in particular, in the case of crystalline semiconductors, can be understood from considerations, which are based on the free ion.

As to the host crystals, the choice of III–V semiconductors, and in particular GaSb, is of key importance because the lattice parameter of this material matches different technologically important solid solutions, whose band gap is in the range between 0.3 and 1.8 eV [3]. In this way GaSb has been successfully applied to the development of novel optoelectronic devices like photodetectors [4], thermophotovoltaic cells [5] and laser diodes [6] operating at 1.5 μm, which is the window of the minimum loss of the silica-based optical fibers.

In this work the defect structure of Er-doped and Te co-doped GaSb samples has been studied. GaSb, which as-grown has p-type behaviour, was intended to be n-type by co-doping with different Te concentrations and introducing Er as oxide (Er_2O_3). The choice of an oxide lies on the fact that previously reported results show that oxygen enhances the luminescence properties of the Er^{+3} ion [7]. The defect structure in these samples was studied by several methods.

2. Experimental details

Three Er-doped and Te co-doped poly-crystalline GaSb ingots being 70 mm in length and 12 mm in diameter were grown in a single-zone rotating Bridgman furnace. The axial thermal gradient was 57 °C cm^{-1}.

* Corresponding author. Tel.: +34-91-3974784; fax: +34-91-3978579.
E-mail address: jl.plaza@uam.es (J.L. Plaza).

0921-5107/02/$ - see front matter
PII: S0921-5107(01)01065-0

As starting material, high purity 99.9999% Ga, Sb and 99.9% Te and Er_2O_3 were used. High quality quartz ampoules were used as crucibles and sealed in vacuum at 10^{-6} Torr. The ampoules were previously graphited by using acetone pyrolysis at 1000 °C in order to prevent the material sticking to the walls. The ingots were grown with three different initial Te concentration in the melt, keeping constant the Er concentration. These concentrations were: Ingot (A): Er (2×10^{19} cm^{-3}), Te (2×10^{19} cm^{-3}), Ingot (B): Er (2×10^{19} cm^{-3}), Te (1×10^{19} cm^{-3}), Ingot (C): Er (2×10^{19} cm^{-3}), Te (4×10^{19} cm^{-3}).

Several wafers where obtained from different positions along the ingots with surfaces perpendicular to the growth direction. For CL and van der Pauw studies, the samples were mechanically polished with 5 and 1 μm alumina powder. The possible oxide layer over the surface of the samples was removed with HCl (37%). Finally a cleaning process with methanol was carried out. For SEM and WDX analysis, an additional etching process for 30 sec with a CP4 type solution (1 CH_3COOH: 5 HF: 9 HNO_3: 10H_2O) applied after mechanical polishing was done.

For the measurement of the resistivity, mobility and carrier density, the van der Pauw technique was used with magnetic fields perpendicular to the samples up to 7 kGauss. These measurements were carried out at room temperature. Indium dots were used as ohmic contacts, which were verified by obtaining ohmic I–V curves.

For the SEM–WDX studies a scanning electron microscope JEOL JM-6400, equipped with a 40 kV electronic microprobe, was used. The CL analysis was carried out using a Hitachi S-500 SEM at accelerating voltages of 20–30 keV. A liquid nitrogen cooled germanium detector was used for signal detection. CL images and spectra presented in this work were obtained at 77 K.

3. Results and discussion

The samples were first analysed by SEM and WDX. The latter technique can be used for microanalysis of elements that are present at very low concentrations (below 0.01% wt.). We start with the analysis of Ingot (A) grown with the same Er and Te initial concentrations in the melt. This analysis has been carried out for several wafers along the ingot. The main differences appear for the samples obtained from the top of the ingot, i.e. the last solidified material, where the cracking of the surface was observed, as shown in Fig. 1, which is attributed to a very high Te concentration which could be present as precipitates. This high Te concentration has been verified by the WDX analysis carried out inside and outside the crack of Fig. 1.

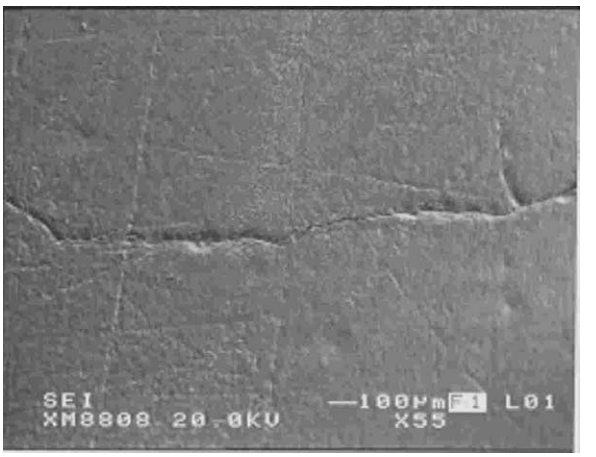

Fig. 1. SEM image from a sample extracted from the latest solidified material of the Ingot (A).

The results of the analysis are the following outside the crack: Ga_{Out} (37.279% at.), Er_{Out} (0.073% at.), Te_{Out} (5.983% at.), Sb_{Out} (56.665% at.). Inside the crack: Ga_{Ins} (30.790% at.), Er_{Ins} (0.064% at.), Te_{Ins} (16.277% at.), Sb_{Ins} (52.869% at.). It is observed that the Te concentration is higher inside the crack. It indicates that Te is preferentially incorporated at the cracks in agreement with the fact that Te tends to appear in higher concentrations at the grain boundaries and defects [9]. It can also be observed that the Er concentration is almost constant on the surface. From these analysis clear evidences of Te accumulation at the final stages of the growth are obtained.

One sample from the middle of the Ingot (A) has also been analysed by WDX along the different grains, which were observed and not shown here for brevity. This chemical analysis does not show significative variations between the concentrations of the elements on the surface of the different grains. It must be pointed out that the resulting Te concentration is much lower than in the previous case.

On the other hand, it has been found that the concentration inside the grain boundaries differs from the values outside. The analysis of one particular grain boundary shows that outside the grain boundary; Ga_{Out} (39.442% at.), Er_{Out} (0.086% at.), Te_{Out} (0.342% at.), Sb_{Out} (60.130% at.) while it was Ga_{Ins} (44.161% at.), Er_{Ins} (not observed), Te_{Ins} (2.402% at.), Sb_{Ins} (53.436% at.) inside the grain boundary. Te concentrations are higher inside the grain boundary. It has been previously demonstrated that Te tends to accumulate at the grain boundaries and dislocations [10].

A similar analysis has been carried out on the Ingot (B) with higher Er than Te initial concentrations in the melt. In this case, we proceed as before beginning with the analysis of one sample from the latest solidified region of the ingot. The WDX analysis has not shown significant differences in the composition of the different

grains. On the other hand it is important to note that, as before, the concentration of Te is higher inside the grain boundaries. In this case it can be noted a higher Er concentration inside the grain boundary ($Er_{Ins} = 0.158\%$ at.), than outside (not observed). It must be pointed out that the Te concentration at the latest solidified region is much lower than in the previous case of Ingot (A) probably due to the fact that in Ingot (B) the initial Te concentration is lower than in the case of Ingot (A).

For comparison, one sample from the middle of the Ingot (B) has been analysed. Fig. 2 shows an image of the surface of this sample obtained by SEM where different grains with parallel grain boundaries can be observed. This kind of defects has been observed in other samples extracted from Ingot (B) and could be related to the particular composition of this ingot because these defects could not be observed in Ingots (A) and (C), the latter one being discussed below.

Several WDX analyses have been carried out in sample (B). The Er concentration inside and outside the regions with these parallel formations (Fig. 2) are the following: Er_{Out} (0.083% at.), Er_{Ins} (0.011% at.). This kind of defects is mainly characterised by an excess of antimony and a slightly lower Er concentration. It must be pointed out that, outside and inside the defects, the Te concentration was zero or below the detection limit.

The CL images from the different ingots also reveal non uniformity of the Te distribution. Fig. 3 shows a CL image of a sample obtained from ingot (A) which shows parallel regions with a set of aligned dots surrounded by a bright halo. This CL contrast of dot and halo is typical for dislocations in III–V semiconductors, indicating an accumulation of nonradiative centers at the dislocation core.

Triangular etch pits with a density around 6×10^4 cm^{-2} have been also observed on the surface. In order to distinguish if the triangular figures were precipitates or dislocations, WDX analysis was carried out outside and inside the etch pits. The results outside were: Ga_{Out}

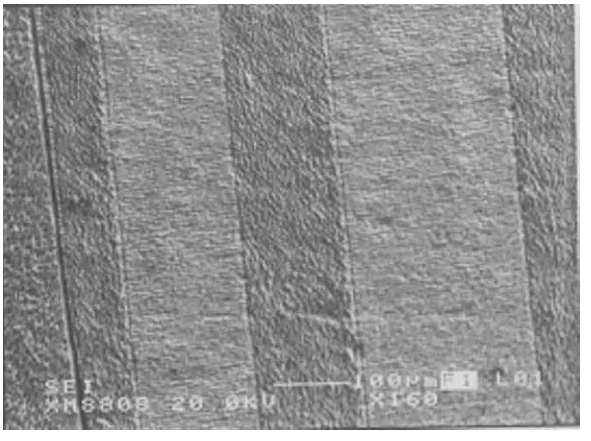

Fig. 2. SEM image from a sample extracted from the middle part of the Ingot (B).

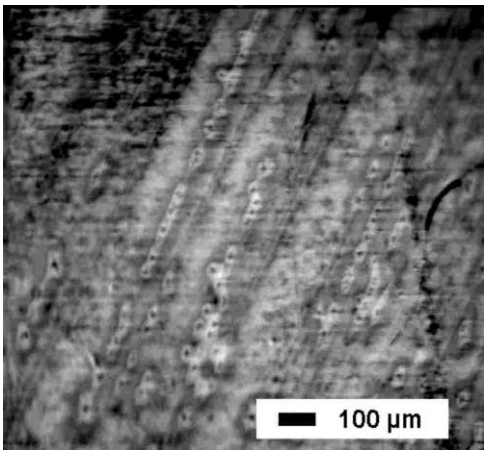

Fig. 3. CL representative image from a sample obtained from the middle part of de Ingot (B).

(43.35% at.), Er_{Out} (0.031% at.), Te_{Out} (not observed), Sb_{Out} (56.620% at.) and inside: Ga_{Ins} (39.024% at.), Er_{Ins} (0.024% at.), Te_{Ins} (0.102% at.), Sb_{Ins} (60.834% at.). The Te concentration is higher inside the defect than outside where it could not be observed. In this way, the low dopant concentration inside indicates that the triangular pits are dislocations and not precipitates. On the other hand, the Er concentration remains almost constant and does not appear to be dependent on the defect structure.

Finally different samples from Ingot (C) with a high Te concentration, were analysed. The WDX analyses give the following values for the concentrations of the different elements: Sb (45.83% at), Te (3.68% at.), Er (1.38% at.), Ga (49.11% at.). The Te concentration is higher than in the previous cases and the concentrations of all the elements are almost constant along the ingot even at the region of the last solidified material. This behaviour, not observed in the other cases, could be due to the presence of Te precipitates, which are homogeneously distributed along the ingot as is revealed by CL images, which show a rather uniform bright background with a high number of small dark dots randomly distributed (Fig. 4).

The CL spectra from all co-doped samples show several emission bands around the band edge energy which are peaked at about 830, 800, 777 and 744 meV. A representative CL spectrum from a co-doped sample is shown in Fig. 5. These bands are related to recombination involving band tail states, Er^{3+} intraionic emission, native acceptors (band A) and a complex defect of Te, respectively. The emission of Er ion is the most important and dominates the CL spectra in all the samples. The intensity level is higher than that obtained in a previous work [8] from GaSb doped only with Er. This result confirms the enhancement of luminescence when Er is surrounded by oxygen, suggested previously in the literature [7]. The 744 meV emission band, intrinsic to Te, is rather weak in the three ingots

Table 1
Resistivity, mobility and electron density from the van der Pauw measurements for the three ingots

Ingot	Resistivity (ohms cm)	Mobility (cm^2 $(Vs)^{-1}$)	Electron density ($\times 10^{18}$ cm^{-3})
A	0.004	400	4.0
B	0.020	200	2.0
C	0.003	800	2.5

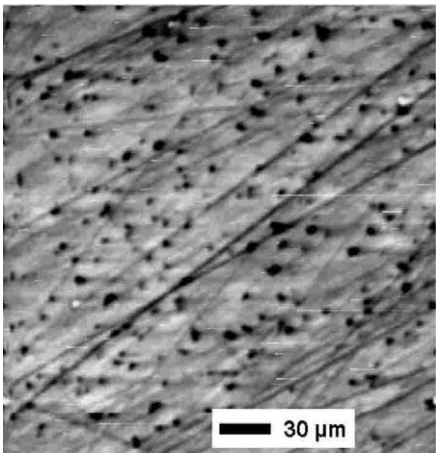

Fig. 4. CL representative image from a sample corresponding to the ingot (C).

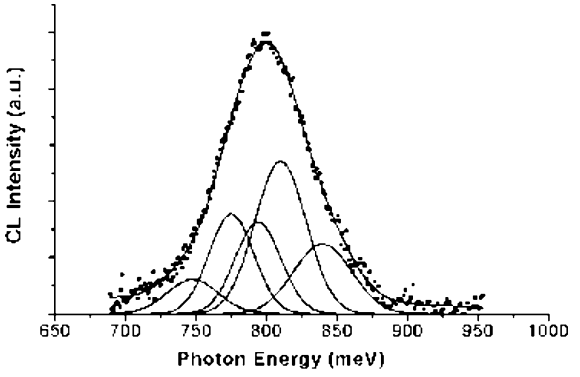

Fig. 5. CL representative spectrum of a sample taken from ingot (B). Points correspond to experimental data and lines correspond to the different emission bands.

investigated. This indicates that at high doping level, Te precipitates and does not contribute to the formation of a complex centre. On the other hand, an increase of the total CL intensity with Te concentration has been detected; thus it seems that co-doping with Te favours Er emission.

The electrical properties of the samples like resistivity, mobility and carrier density have been obtained by the van der Pauw technique. All the samples resulted to be n-type meaning that in all the cases, even when the initial concentration of Er was higher than Te, the Er does not compensate the donor Te impurities, probably due to the fact that Te is more effectively incorporated in the GaSb matrix than Er. It is supported by the WDX analysis, which in almost all cases show a higher Te than Er concentration. Different samples along the ingots were analysed giving the values shown in Table 1. These are mean values, because the particular values of the electrical properties of each sample depend on the position because of dopant differences induced by axial segregation effects along the ingot. From these values it can be observed that the mobility increases with the Te concentration. This is in accordance with the decrease in the resistivity. On the other hand, it can be observed that the resistivity is high corresponding also with the case of low electron concentration and lower Te concentration. These results suggest a critical relation between Er and Te initial concentrations in the melt corresponding to Ingot (A) where the carrier density is the highest for the three cases.

4. Conclusions

Three different Er-doped and Te co-doped GaSb ingots have been analysed by means of SEM, WDX, CL and van der Pauw technique. In the case of the same Er and Te initial concentrations in the melt, Te is mostly located at the latest solidified material.

It has been observed that Te is preferentially located at the dislocations and grain boundaries. This does not seem to be the case for Er, which is located almost in the same concentration along the ingots. An increase of the total CL intensity with Te concentration has also been observed. From this behaviour it could be said that co-doping with Te favours Er emission.

The van der Pauw measurements give an n-type behaviour in all the samples showing a critical relation of the Er–Te initial concentrations in the melt with a high electron density corresponding to the case of equal Te and Er initial concentration in the melt.

References

[1] W.H. Haydl, H.D. Müller, H. Ennen, W. Korber, K.W. Benz, Appl. Phys. Lett. 46 (9) (1985) 870.
[2] L. Smentek, Phys. Rep. 297 (1998) 155.
[3] A.G. Milnes, A.Y. Polyakov, Sol. Stat. Electron 36 (1993) 803.

[4] O. Hildebrand, W. Kuebart, K.W. Benz, M.H. Pilkuhn, IEEE J. Quatum Electron QE-17 (1981) 284.
[5] L.M. Frass, G.R. Girard, J.E. Avery, B.A. Arau, V.S. Sundaram, A.G. Thompson, J.M. Gee, J. Appl. Phys. 66 (1989) 3866.
[6] G. Motosugi, T. Kagawa, Jpn. J. Appl. Phys. 19 (1980) 2303.
[7] J.M. Zavada, D. Zhang, Sol. Stat. Electron 387 (1995) 1285.
[8] P. Hidalgo, B. Mendez, J. Piqueras, J.L. Plaza, E. Dieguez, Semicond. Sci. Technol. 13 (1998) 1431.
[9] P.S. Dutta, B. Mendez, J. Piqueras, E. Dieguez, H.L. Bhat, J. Appl. Phys. 80 (1996) 1112.
[10] J.L. Plaza, Ph.D Thesis, Universidad Autonoma of Madrid (2001).